ORIGINAL PAPER

Experimental investigation on dynamic mechanical characteristics and fracture mechanism of coal under repeated impact loads

Kai Wang[1,2] · Guorui Feng[1,2] · Tingye Qi[1,2] · Jinwen Bai[1,2] · Yujiang Zhang[1,2] · Jun Guo[1,2] · Cheng Song[1,2] · Boqiang Cui[1,2]

Abstract

In underground coal mining, frequent dynamic disturbances adversely affect the stability of coal pillars. Thus, it is essential to understand the dynamic mechanical behaviour of coal under repeated impact loads. In this paper, a cone-shaped striker bar with a length of 200 mm was designed for a split Hopkinson pressure bar (SHPB) system, and repeated impact experiments of coal were carried out with this system. Based on three-wave theory, original voltage signals were recorded during the tests and then processed to study the changes in the dynamic stress-strain curves with the number of impacts. Relationships between the dynamic compressive strength, peak strain, and the number of impacts were analysed. Meanwhile, the failure mode and fracture mechanism of coal under repeated impact loads were discussed. It was found that as the number of impacts increases, the peak strain increases but the dynamic strength decreases. Furthermore, the studied coal specimens present two typical failure modes under these conditions, including axial splitting failure and hoop tensile failure. Based on the ultimate fracture modes of the specimens, two crack group failure models are established to reveal the fracture mechanism of coal under repeated impact loads. This study can make a deep understanding about the failure mechanism of coal pillar's instability induced by impact load.

Keywords Coal · Repeated impact loads · Mechanical characteristics · Fracture mechanism · Spilt Hopkinson pressure bar

Introduction

In the 1980s, room and pillar mining methods were primarily utilized to extract coal seams in most coal mines in China (Zhang et al. 2016). This mining method abandoned a large quantity of coal pillars, especially in the Shendong and Datong mines, China (Bai et al. 2019; Zhang et al. 2019). The dynamic failure of remnant coal pillars can easily induce goaf collapse and surface subsidence (Xu et al. 2017). For this reason, many experts and scholars have conducted extensive research on the failure mechanism of coal or rock pillars (Cao et al. 2016; Cording et al. 2015; Wang et al. 2011; Yang et al. 2015; Zhou et al. 2018; Zhu et al. 2017). In practical mining engineering, remnant coal pillars are more vulnerable to frequent dynamic disturbances, such as dynamic loads induced by hard stratum fracture, blasting stress concentration coal pillars, fault activation, and roadway excavation, as shown in Fig. 1. These frequent dynamic loads may degrade the bearing capacity of the coal and even induce the instantaneous collapse of the coal pillars. According to previous studies investigated by many scholars, frequent dynamic disturbances can be simplified to a kind of repeated impact load in the laboratory (Li et al. 2011; Li et al. 2005; Ramulu et al. 2009; Xiao et al. 2009). Therefore, investigating the dynamic mechanical behaviour of coal under repeated impact loads is fundamental to comprehensively understanding the failure mechanism of remnant coal pillars.

According to the recommendations of the International Association of Rock Mechanics (Zhou et al. 2012), the SHPB system has been used as an important and reliable device for studying the mechanical behaviour of rock material under dynamic loads. Hence, extensive tests have
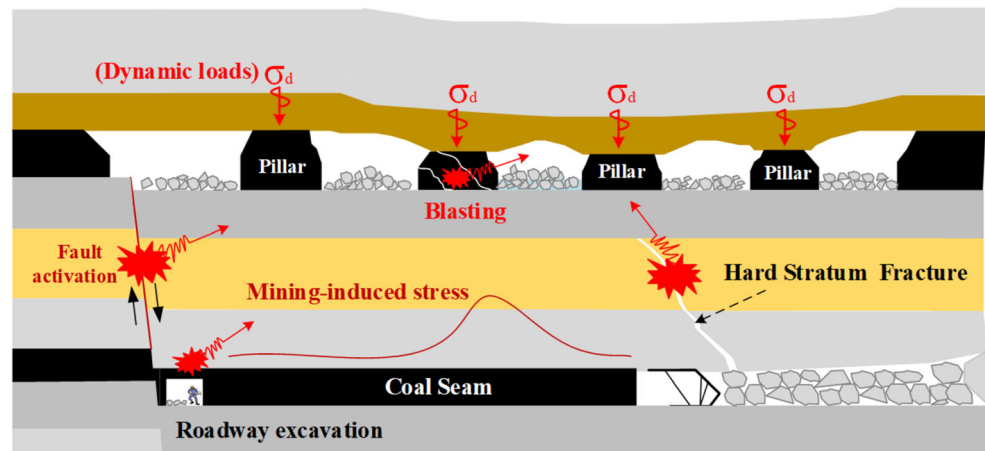
✉ Guorui Feng
  fguorui@163.com

✉ Tingye Qi
  qty198402@163.com

1   College of Mining Engineering, Taiyuan University of Technology, Taiyuan 030024, China

2   Research Center of Green Mining Engineering Technology in Shanxi Province, Taiyuan 030024, China

Fig. 1 Dynamic stress environment of remnant coal pillars

been performed using a modified SHPB system to study the dynamic mechanical behaviour of rock materials under repeated impact loads. Jin et al. (2013) investigated the effects of repeated impact loads on the energy dissipation and failure mechanism of sandstone. The conclusions provide useful references for the blasting design of rock engineering. Furthermore, an evolution model of damage accumulation was established to explain the damage characteristics of sandstone under repeated impact loads (Jin et al. 2014). Tang et al. (2015) studied the mechanical properties of skarns under one-dimensional coupled static and repeated impact loads, and found that rock has fatigue damage characteristics. Moreover, many constitutive equations have also been proposed (Wang et al. 2017; Zhu et al. 2013), which comprehensively consider the effects of axial static loads, repeated impact loads, and confining pressure on the deformation of rock. Most recently, some geophysics methods, such as acoustic emission (Li et al. 2018) and scanning electron microscopy (Shu et al. 2019), have also been applied to study the rock fracture mechanism under repeated impact loads.

Coal is a special rock material with a large number of natural fissures. Compared with other hard rocks, coal has a relatively low strength. It is more challenging to apply a repeated impact loading on coal using the SHPB system. Therefore, the previous studies associated with the dynamic mechanical behaviour of coal mostly focused on a single impact load using the SHPB system. For instance, Klepaczko et al. (1984) first studied the mechanical characteristics of coal under impact loads, and found that the dynamic mechanical parameters of coal were significantly influenced by the strain rate. Shan et al. (2006) studied the deformation characteristics of anthracite samples at high strain rates and found that the dynamic stress-strain curves could be mainly divided into four stages. Li et al. (2016) studied the magnetic field characteristics of coal under different impact velocities, and found that the signal amplitude of the transient magnetic field changes with the limit of the value of the fracture stress during the impact failure process. Meanwhile, more efforts have been

devoted to investigating the dynamic mechanical properties of coal, taking into consideration the effects of water content (Wang et al. 2016; Zhao et al. 2016), temperature (Yin et al. 2016), and gas pressure (Kong et al. 2019; Yin et al. 2019).

A review of previous studies suggests that the mechanical properties, deformation characteristics, and constitutive equations of various rocks under repeated impact loads have been explored extensively. Studies of coal materials have thus far mostly focused on their mechanical responses under single impact load. However, the dynamic mechanical behaviour of coal, in terms of metrics such as the stress-strain curve, failure mode, and fracture mechanism under repeated impact loads, is not clear. In this paper, a cone-shaped striker bar with a length of 200 mm was designed, and repeated impact experiments of coal specimens were carried out successfully with this system. Based on the experimental data, the relationships between the dynamic strength, deformation characteristics, and number of impacts were analysed. More specifically, the changes in dynamic stress-strain curves with the number of impacts were discussed. Finally, the crack propagation and failure modes of coal under repeated impact loads were explored, based on which two failure models were established to reveal the fracture mechanism of this coal under these conditions. The results of this study can provide a theoretical basis for the safe mining of coal resources and the prevention of dynamic disasters.

Experimental work

Coal specimen preparation

Fresh coal blocks were collected from the 8117 working face of the Majiliang Mine, Datong city, Shanxi Province, China. According to the experimental methods suggested by the International Society of Rock Mechanics (ISRM 1978; Zhou et al. 2012), the experimental coal specimens were made into cylinders with a diameter of 50 mm and a height of 30 mm. To

remove the friction phenomenon and reduce the transmission wave error, the roughness and the perpendicularity of the two loading planes were both less than 0.02 mm after cutting and polishing. Moreover, the NM-4B non-metal ultrasonic testing system was used to measure the wave velocity of the prepared specimens. Finally, ten specimens were picked and numbered (D1–D10). The locations of the Majiliang mine and prepared coal specimens are shown in Fig. 2. Before carrying out the impact test, the basic mechanical parameters of the coal specimens were measured, as shown in Table 1.

Experimental system

According to the recommendations of the International Society of Rock Mechanics (Zhou et al. 2012), the Hopkinson pressure bar (SHPB) test system has been extensively used as reliable equipment for studying the mechanical response of rocks under high strain rate conditions. In this study, a split Hopkinson pressure bar (SHPB) system was employed to conduct repeated impact experiments on coal specimens. The testing system includes three bars (a striker bar, an incident bar, and a transmission bar), an ultra-dynamic strain instrument, an oscilloscope, a data processing system, and an air compressor, as shown in Fig. 3. The incident bar, transmission bar, and striker bar used in the experiments are all made of 7075 aluminium alloy (see Fig. 4(a)). The diameters of the incident bar and transmission bar are 50mm, while the lengths of these bars are both 2500mm. The detailed physical and mechanical parameters are shown in Table 2.

The main purpose of the dynamic experiments is to realize repeated impact loading of the coal specimens. Therefore, before subjecting the specimen to repeated impact loading conditions, it is important to guarantee that macrofractures are not produced in the specimens after the first impact. For this reason, the methods of reducing the size of the striker bar and shortening the impact distance were adopted to reduce the impact energy loaded on the specimen. Specifically, an aluminium alloy striker bar with a length of 200 mm was designed, as shown in Fig. 4(b). Compared with the alloy steel striker bar used in previous experiments (Cai et al. 2020; Jin et al. 2014; Wang et al. 2016; Yin et al. 2016; Zhao et al. 2016), the size of this aluminium alloy striker bar is relatively small, and this bar can produce an impact with less kinetic energy. In addition, the source of the impact pressure is an air compressor (see Fig. 4(c)). The accuracy of the air

compressor can be controlled within 0.02MPa. Based on previous trials, macrofracture of the coal specimens cannot occur when the impact pressure is 0.06 MPa. Therefore, 0.06 MPa is determined as the impact gas pressure for this experiment.

Experimental theory

Previous studies have shown that an input strain wave $\varepsilon_i(t)$ and reflected strain wave $\varepsilon_r(t)$ are generated in the incident bar. Meanwhile, a transmission strain wave $\varepsilon_t(t)$ is generated in the transmission bar (Li et al. 2008; Xia and Yao 2015). Therefore, the strain gauges were affixed on the incident and transmission bars to record the three elastic waves, which were in turn connected to an ultra-dynamic strain instrument, an oscilloscope, and a data processing system. Based on three-wave theory (Mohr et al. 2010), the strain rate, strain, and stress of the specimen can be calculated by Eqs. (1) to (3):

$$\dot{\varepsilon}(t) = \frac{C}{L_s}[\varepsilon_i(t) - \varepsilon_r(t) - \varepsilon_t(t)] \tag{1}$$

$$\varepsilon(t) = \frac{C}{L_s}\int_0^t [\varepsilon_i(t) - \varepsilon_r(t) - \varepsilon_t(t)]dt \tag{2}$$

$$\sigma(t) = \frac{A}{2A_s}E[\varepsilon_i(t) + \varepsilon_r(t) + \varepsilon_t(t)] \tag{3}$$

where $\varepsilon(t)$ is the strain of the specimen; $\sigma(t)$ is the stress of the specimen; $\dot{\varepsilon}(t)$ is the strain rate of the specimen; C is the velocity of the stress wave propagation in the elastic bar; t is the duration of the stress wave pulse; L_s and A_s are the length and the sectional area of the specimen, respectively; and E and A are the elastic modulus and the sectional area of the elastic bar respectively. Specifically, the determination of the dynamic peak stress and strain rate of the specimen is shown in Fig. 5.

Experimental process

The repeated impact tests of the coal specimens mainly included the following steps: (1) Before each impact test, the coal specimen was sandwiched between the incident bar and transmission bar. Vaseline was applied between bars and specimen to reduce the effect of interface friction. (2) It was checked that the striker bar was in the same position before each impact test. Hence, the striker bar was placed 100 mm from the outlet of the chamber, as shown in Fig. 3. (3) The

Table 1 Basic mechanical parameters of the coal specimens

Specimen	Uniaxial compressive strength (MPa)	Elastic modulus (GPa)	Compressional wave velocity (m/s)	Poisson's ratio	Density (kg/m³)
Coal	9	2.33	1985	0.45	1358

Fig. 2 Location of the Majiliang coal mine and coal specimens
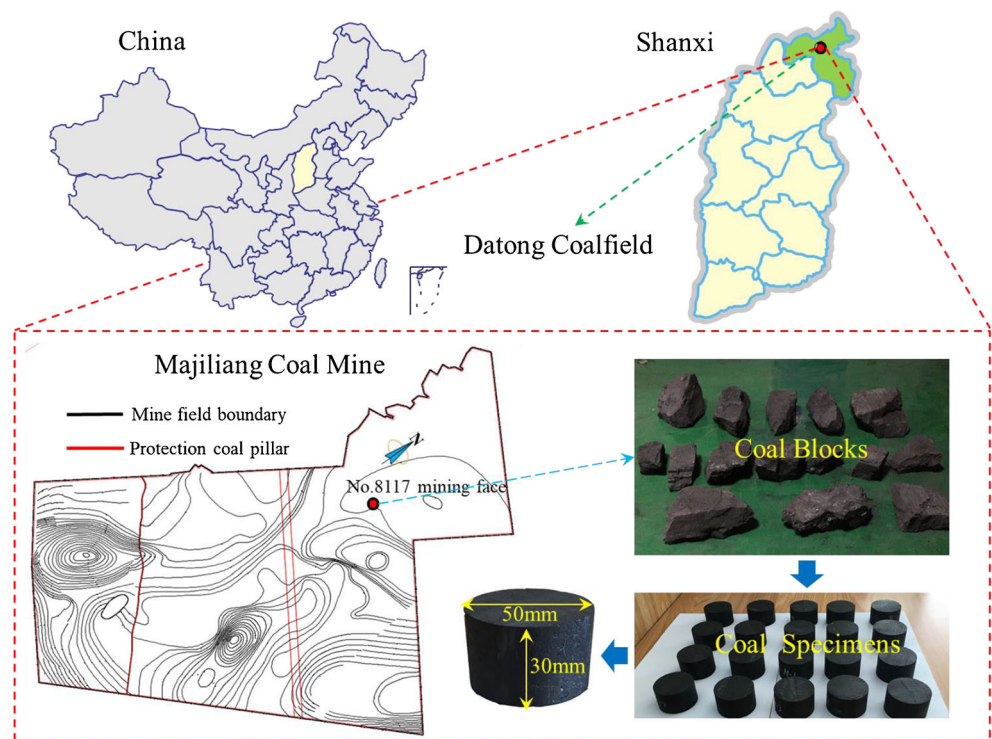
pressure value of the pressure gauge (see Fig. 4(d)) was set to 0.06 MPa so that the high-pressure air drives the striker bar to hit the incident bar and trigger the first impact on the specimen. (4) After the first impact was applied to the specimen, whether the specimen had been macroscopically fractured and lost its bearing capacity was checked. Then, the impact loads were continued until the specimen eventually failed.

Experimental results and analysis

Characteristics of the dynamic stress wave

During the dynamic experiments, the raw voltage signals were collected using an ultra-dynamic strain instrument. The typical dynamic stress wave signals are depicted in Fig. 6. A similar half-sine incident wave was generated by using a cone-shaped striker bar with a length of 200mm. Previous studies have verified that a similar half-sine incident wave can alleviate high-frequency oscillations and achieve better stress uniformity within a short time (Davies and Hunter 1963; Zhang and Zhao 2014). Moreover, the duration of the incident wave from the action of impact loading to completion of loading on the specimen is approximately 120μs. The amplitude of the incident wave for each impact load is almost the same.

The reliability of the SHPB test results will be affected by waveform dispersion and inertia effects. Therefore, realizing the dynamic stress balance on the two end faces of the specimen is a prerequisite to ensure the validity of the SHPB test results. (Dai et al. 2010). In this study, the dynamic stress equilibria are checked for all specimens. Figure 7 shows the typical dynamic stress balance verification curve of the specimen. The sum of the incident stress wave and the reflected stress wave is almost consistent with the transmitted stress wave, which indicates that the experiments satisfy the requirements of the SHPB test.

The representative dynamic stress-strain curves

Figure 8 shows the typical stress-strain curves of specimens under repeated impact loads. The changing features of the

Table 2 The physical and mechanical properties of the SHPB

Material	Diameter (mm)	Young's modulus (GPa)	Compressional wave velocity (m/s)	Poisson's ratio	Density (kg/m³)	Elastic limit (MPa)
7075 Al alloy	50	71	5000	0.3	2810	455

**Fig. 3** Schematic diagram of SHPB test system
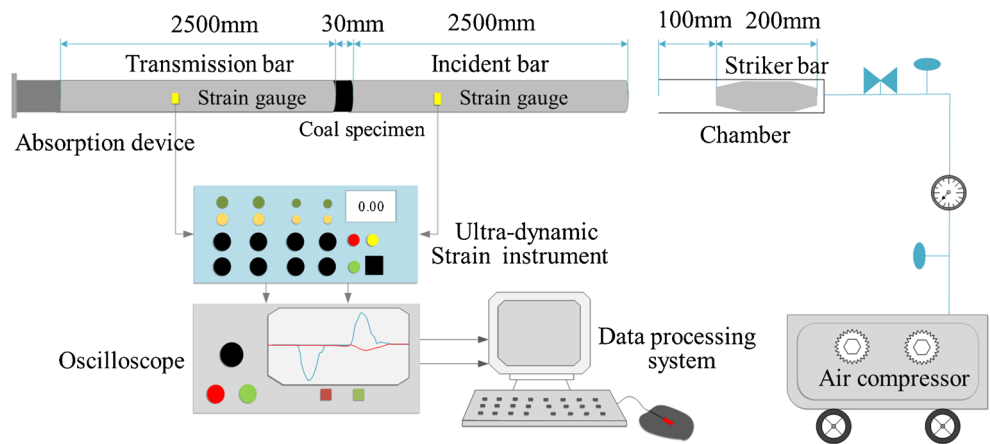
stress-strain curves between the first impact and the second impact were analysed, as shown in Fig. 9. The following characteristics were identified:

(1) During the first impact and the second impact, the specimen deformations consist of four stages: ① Extremely short compaction state (*OA*, *OA′*). In this stage, there are no obvious compaction phenomena under repeated impact loads. ② Microcrack stable propagation stage (*AB*, *A′B′*). In this stage, the strain increases linearly with the stress. ③ Microcrack unstable propagation stage (*BC*, *B′C′*). Under the continuous action of the stress wave, the coal specimen begins to experience nonlinear deformation. ④ Stress unloading stage (*CE*, *C′E′*). This stage consists of two parts: the first is an unloading stage (*CD*, *C′D′*), and the second is an unloading stage (*DE*, *D′E′*).

(2) The slopes of the stress-strain curve are different between the first impact and the second impact. The curves of the initial loading phase (*OA*, *OA′*) are almost completely

Fig. 4 The testing system of SHPB: **a** incident bar and transmission bar, **b** striker bar, **c** air compressor, **d** pressure gauge
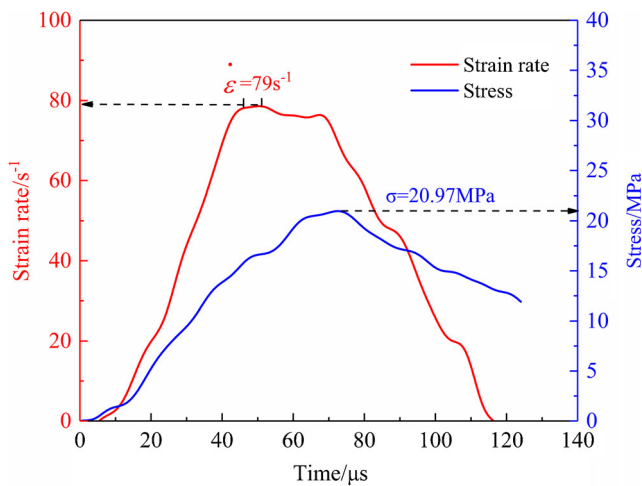

(a)

(b)

(c)

(d)
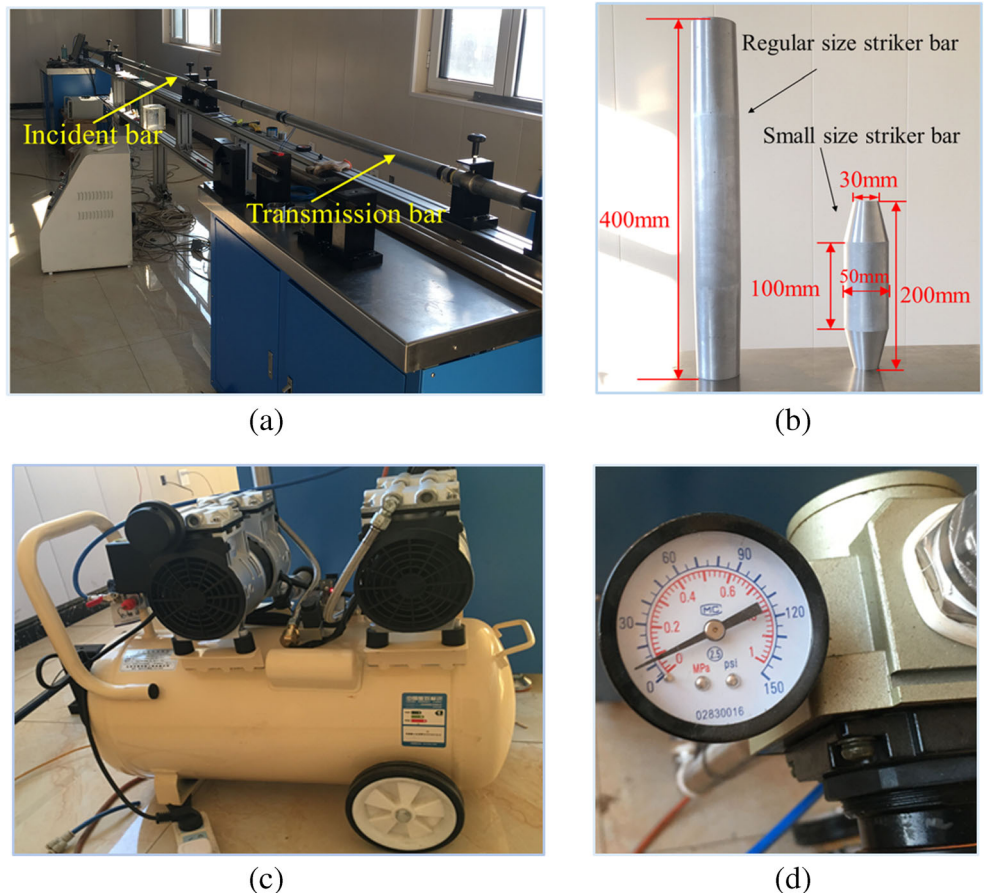
Fig. 5 Determination of strain rate and dynamic strength
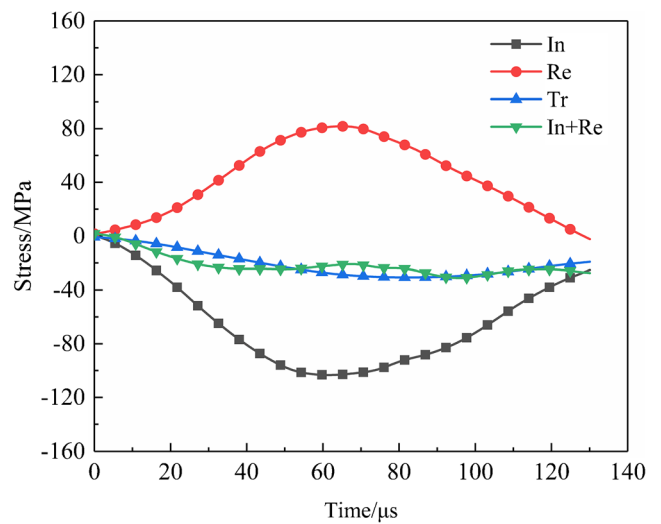

Fig. 7 Verification of the dynamic stress equilibrium of a specimen

coincident, indicating that the initial elastic moduli of the coal specimens are almost the same. However, in the elastic deformation stage (AB, A′B′) and the inelastic deformation stage (BC, B′C′), the slopes of the curves both decrease with an increasing number of impacts. This can be explained as follows: The coal specimen experiences a certain degree of damage under the first impact load. The propagation of internal microcracks leads to a reduction in the transmission efficiency of the stress wave inside the specimen.

(3) The shapes of the first two stress-strain curves are almost similar from the origin to the peak stress point (OC, OC′), indicating that the second impact load does not

change the constitutive characteristics of the loading section. However, there are some differences between sections DE and D′E′. An obvious "strain rebound" phenomenon exists during the unloading state (DE). This is because macrofractures in the coal specimens are not produced after the first impact and the release of elastic energy causes the strain to rebound. Then, the curve of the unloading section (D′E′) significantly slows down, and the "strain rebound" disappears. This indicates that the increase in damage inside the specimen results in the reduction in the elastic deformation after the second impact.

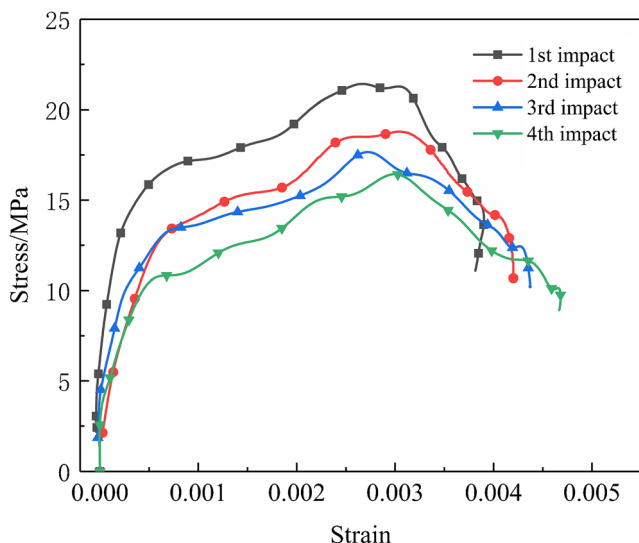Fig. 6 Typical stress wave signals under repeated impact loads
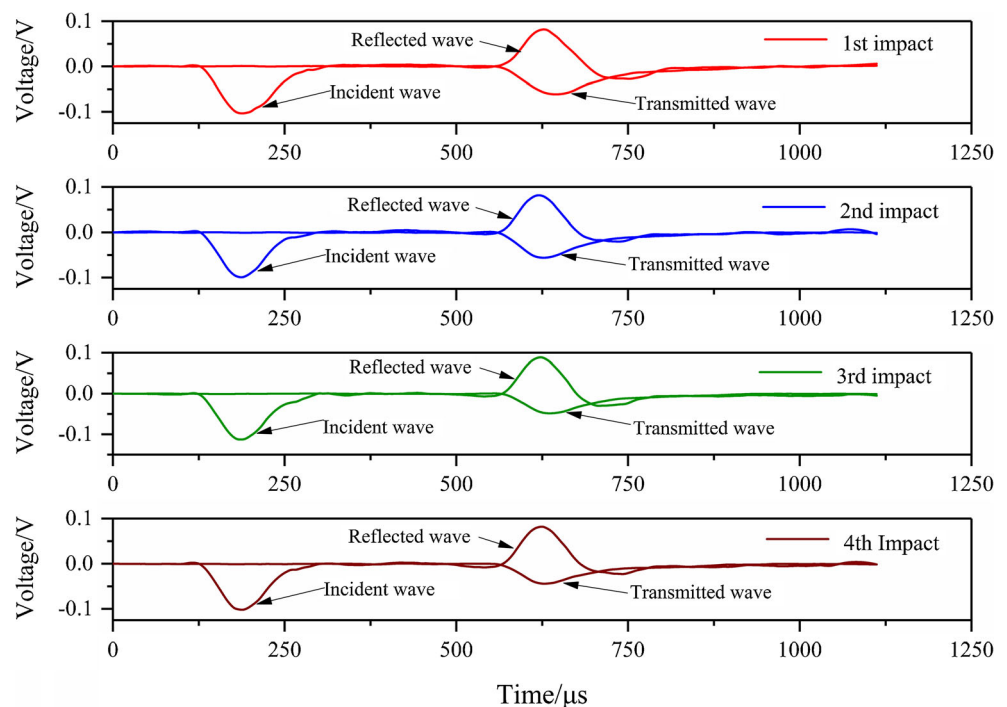
Fig. 8 Stress-strain curves under repeated impact loads

Changes in the dynamic strength with increasing number of impacts

In this study, the related dynamic experimental results of coal specimens are listed in Table 3. To study the dynamic strength characteristics of coal under repeated impact loads, the relationships between the dynamic peak stress and the number of impacts are further analysed. As shown in Fig. 10, the average dynamic peak stress of the coal specimens shows a decreasing trend with increasing impact number. More specifically, the degradation coefficient of dynamic peak stress is defined to quantify the damage degree of coals under repeated impact loads. The degradation coefficient of the dynamic peak stress can be expressed by Eq. (4).

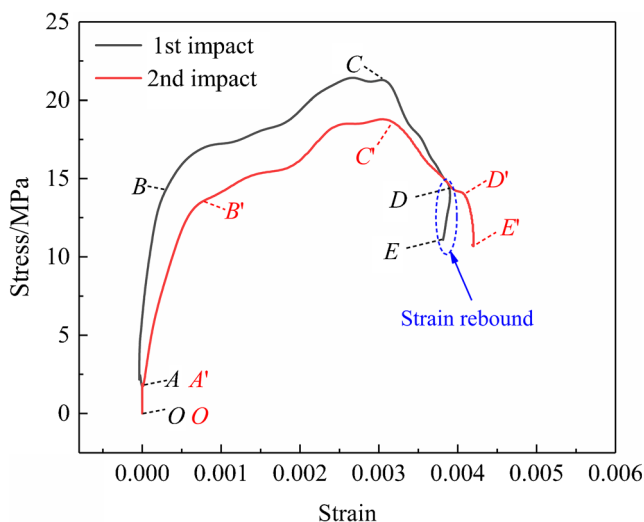$$\delta_\sigma = \frac{\sigma_0 - \sigma_f}{\sigma_0} \times 100\% \tag{4}$$

Fig. 9 Changes in the dynamic stress-strain curves with increasing number of impacts

where δ_σ is the dynamic peak stress degradation coefficient, σ_0 is the peak stress of the first impact, and σ_f is the peak stress of the last impact.

The calculated result shows that the degradation coefficients of this coal range from 0.20 to 0.37, with an average value of 0.29. These findings are similar to those of sandstone (Jin et al. 2012). Based on the above analysis, it can be concluded that the number of dynamic disturbances has a significant influence on the ability of coal to resist impact loads.

Changes in the deformation with increasing number of impacts

Coal rock inevitably deforms during the impact loading process, which mainly transitions from microscopic accumulative damage to macroscopic fracture. Therefore, it is important to investigate the deformation changes with the number of impacts. Figure 11 shows four strain-time curves of the D-6 specimen under repeated impact loads. On the one hand, the four curves all have the same characteristics: the slope of the strain with time remains almost unchanged during the initial loading stage. Then, the strain increases rapidly and reaches the peak value. On the other hand, the slope of the strain versus time curve shows an increasing trend with the increase in the impact numbers.

Moreover, the relationships between the peak strain and the number of impacts are also summarized to further investigate the deformation characteristics of these specimens under repeated impact loads. As shown in Fig. 12, the average peak strain of the coal specimens increases with increasing impact number. This indicates that the capacity of coal to resist impact deformation decreases with increasing impact number. Meanwhile, this result also reveals that damage can be easily produced inside the coal body under repeated impact loads. Therefore, it can be concluded that frequent dynamic disturbances can degrade the bearing capacity of coal rock and even induce the instability of coal pillars.

Coal is a typical sedimentary rock (Wang et al. 2020). Mineral grains and other land-based debris constitute the skeleton structure of the coal body. Organic matter, cements, and other fine-grained debris constitute the filler (called the "matrix") of the coal skeleton structure. A single impact cannot cause a macrofracture to form in the coal rock, but the internal matrix and skeleton structure begin to break. After repeated impacts, the macrocracks start to nucleate and expand until breakthrough. The response to this deformation is that the strain of the coal gradually increases with increasing impact number.

Crack propagation and failure modes

Under the action of repeated impact loads, crack initiation, propagation, and coalescence cause the coal specimens to

Table 3 Experimental results of the coal specimens under repeated impact loads

Numbers	strain rate/s^{-1}	Dynamic peak stress/MPa	Dynamic peak strain
D-1-I	79	20.97	0.005015
D-1-II	79.64	16.98	0.005607
D-2-I	75.54	19.63	0.004219
D-2-II	107.61	14.51	0.004882
D-4-I	52.76	21.73	0.002916
D-4-II	61.55	18.42	0.003709
D-4-III	54.26	17.39	0.003909
D-5-I	48.52	12.33	0.002827
D-5-II	51.24	10.37	0.003643
D-5-III	51.55	8.85	0.003687
D-5-IV	52.77	8.63	0.003988
D-6-I	79.71	21.42	0.003902
D-6-II	86.76	18.79	0.004373
D-6-III	78.81	17.66	0.004680
D-6-IV	80.68	16.44	0.004952
D-7-I	62.78	17.28	0.003341
D-7-II	96.54	11.00	0.005558
D-7-III	96.30	10.84	0.005700
D-8-I	57.21	19.22	0.002916
D-8-II	71.33	18.88	0.003525
D-8-III	73.27	12.60	0.005432
D-10-I	76.24	15.32	0.004392
D-10-II	69.74	12.79	0.003920
D-10-III	73.73	11.51	0.004337
D-10-IV	96.99	10.83	0.006203

Note: *D*, dynamic experiment; *(1–10)*, the specimen number; *(I–IV)*, the number of impacts.

become damaged and undergo failure. The evolution of cracks can not only reflect the failure process of the coal, but can also be useful for understanding the failure mechanism of coal pillars. Table 4 shows the crack evolution photographs of
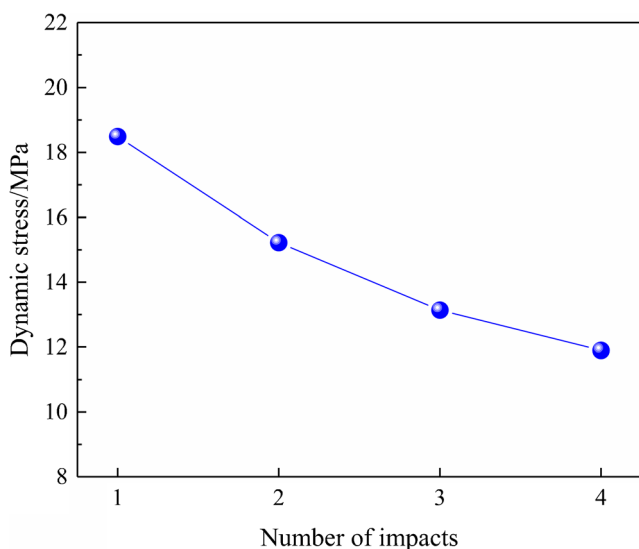
specimens under repeated impact loads, taking specimens D-4, D-5, D-6, D-7, and D-8 as examples. Among them, specimen D-5 underwent four impact loadings during the failure process. The entire specimen was still intact after the first impact, and only a main axial tensile crack (TC-1) was produced along the end surface of the specimen. After the second and third impacts, TC-1 continued to expand, while a microfracture (MF) was produced at the left edge of the specimen. After the fourth impact, another main axial tensile crack (TC-2) was produced below TC-1. The two axial tensile cracks caused macroscopic fracture of the entire specimen. The bearing capacity of the coal specimen was eventually lost. It should be noted that D-4, D-7, and D-8 were destroyed after the third impact. The crack evolutions of D-4 and D-7 are similar to those of D-5. However, D-8 exhibited composite failure mode due to hoop and axial tensile cracks. After the first impact, there was no obvious damage on the surface of the D-8. However, a macroscopic hoop tensile crack was produced in the middle of the specimen due to second impact. In addition, two axial penetrating cracks were produced after the third impact. They formed to the upper left and lower right of the hoop tensile crack. Finally, the axial penetrating cracks and hoop tensile crack crossed and propagated, which caused macroscopic fracture of the entire specimen.

Discussion

In the previous section, the changing features of the dynamic strength and deformation with the number of impacts were analysed. In the following section, the fracture mechanism of coal affected by repeated impact loads will be discussed.
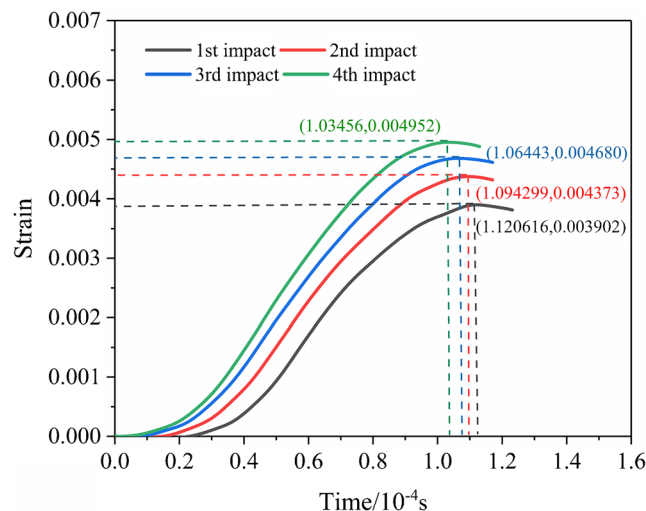

Fig. 10 The relationship between the peak stress and the number of impacts

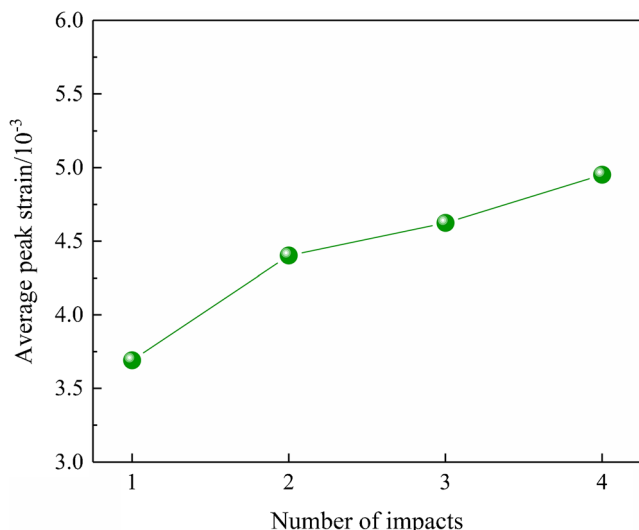**Fig. 11** Changes in strain with time under repeated impact loads

Fig. 12 The relationship between the peak strain and number of impacts

The influencing factors of the fracture formation in coal

Coal is a porous medium with a large number of original cracks randomly distributed in all directions (Zhao et al. 2016). Under the action of dynamic stress waves, stress concentration inevitably occurs at the crack tips. On the one hand, when the stress intensity factor (SIF) at a crack tip reaches the fracture toughness, the crack begins to expand (Wang and Shrive 1995). On the other hand, when a crack propagates to a certain length, the adjacent cracks will be affected, which means that these cracks will gradually coalesce and form macroscopic ruptures (Wong and Einstein 2009a, 2009b). Therefore, the interaction between the crack groups should be considered an important factor of the failure of the specimen (Horii and Nemat-Nasser 1985, 1986).

From the above experiments, the crack propagation characteristics of the studied coal are shown in Table 4. It is found that these coal specimens produce two types of tensile cracks (axial tensile cracks and hoop tensile cracks) that are parallel and perpendicular to the axial stress, respectively. This indicates that the original axial tensile crack and transverse tensile crack are the main cracks dominating the failure of the specimen. These two types of cracks correspond to the axial tensile failure and hoop tensile failure of the coal specimens, respectively, as shown in Fig. 13.

Therefore, the influencing factors of the formation of fracture in coal include not only external factors but also internal factors, as shown in Fig. 14. The external influence factors are the repeated impact loads. The internal influencing factors are the original axial crack group and the transverse crack group inside the coal.

Two failure models of the crack group

To better reveal the fracture mechanism of coal under the influence of the two main aforementioned factors, two failure models of the crack group were established based on the slip crack model (Horii and Nemat-Nasser 1986). The axial crack group failure model and transverse crack group failure model are depicted in Fig. 15 (a) and Fig. 15 (b), respectively. Moreover, the force diagram of the models can be simplified, as shown in Fig. 15 (c) (Li et al. 2000).

According to the theory of dynamic fracture mechanics (Freund 1990; Li et al. 2000), the dynamic stress intensity factor (K_{ID}) of the crack tip for the models of the axial crack group and transverse crack group can be expressed by Eq. (5) and Eq. (6), respectively:

$$K_{ID} = k(v)K_I = k(v)\frac{F_d\sin\theta}{\sqrt{w\sin\left[w\sin\left[\pi(l + l^*)\right]/w\right]}} \quad (5)$$

$$K_{ID} = k(v)K_I = k(v)\sigma\sqrt{2w\tan(\pi c/2w)} \quad (6)$$

where K_{ID} is the dynamic stress intensity factor; K_I is the static stress intensity factor; $K(v)$ is a constant function of crack growth velocity (v); θ is the angle between the wing crack and the principal stress; l is the wing crack length; l^* is equal to $0.27c$; c is the crack half-length; w is the wing crack centre distance; and F_d is the driving force of crack growth, and its calculation formula is as follows (Li et al. 2000):

$$F_d = 2c\sigma\left(\sin\theta\cos\theta - \mu\cos^2\theta\right) \quad (7)$$

where σ is the dynamic compressive stress and μ is the coefficient of friction. According to the previous study by Freund (1990), $K(v)$ can be expressed as follows:
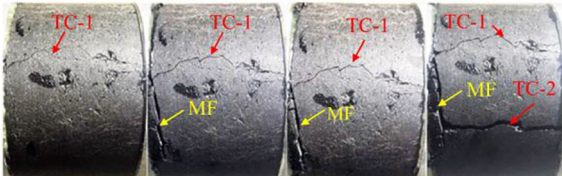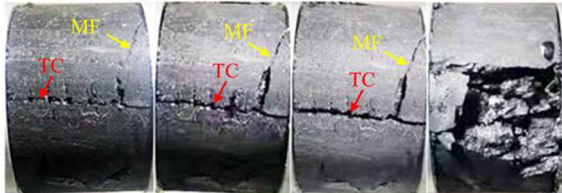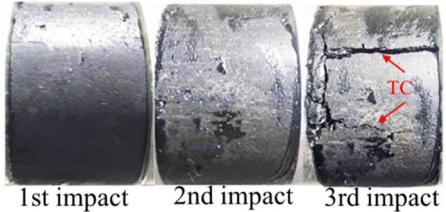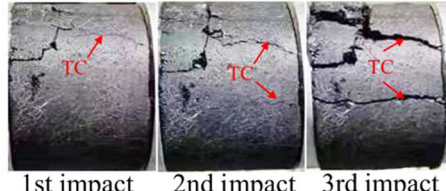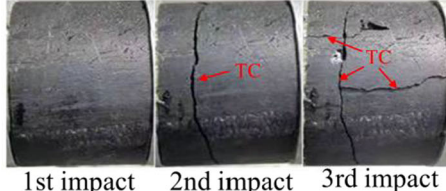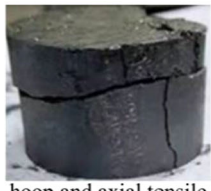
$$k(v) = \frac{v_R - v}{v_R - 0.75v} \quad (8)$$

where v_R is the Rayleigh wave velocity. Combining Eqs. (5) to (8), the dynamic speed of the wing crack growth (v) can be expressed as follows:

$$v = \frac{dL}{dt} = \frac{1 - A}{1 - 0.75A}v_R \quad (9)$$

where L is the instantaneous length of the wing crack and A is the ratio of the dynamic fracture toughness to the static stress intensity factor of the sliding crack group model. The increased length of the axial crack group and transverse crack group of the specimen during each impact load can be recorded as $L_i(i = 1, 2, 3...)$, which can be calculated by Eq. (10) and Eq. (11) respectively:

Table 4 Crack evolution of coal specimens under repeated impacts

Specimen	Impact numbers	Cracks evolution photos	Ultimate failure modes
D-5	4	1st impact 2nd impact 3rd impact 4th impact	axial tensile failure
D-6	4	1st impact 2nd impact 3rd impact 4th impact	axial tensile failure
D-4	3	1st impact 2nd impact 3rd impact	axial tensile failure
D-7	3	1st impact 2nd impact 3rd impact	axial tensile failure
D-8	3	1st impact 2nd impact 3rd impact	hoop and axial tensile composite failure

Note: *TC* represents tensile crack; *MF* represents micro-fracture.

Fig. 13 Typical failure modes of coal specimens: **a** axial tensile failure, **b** hoop tensile failure
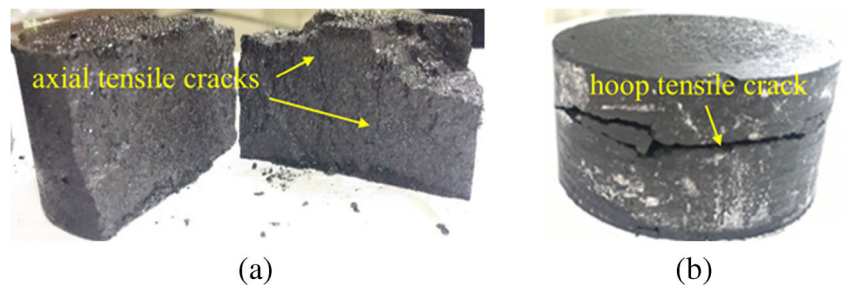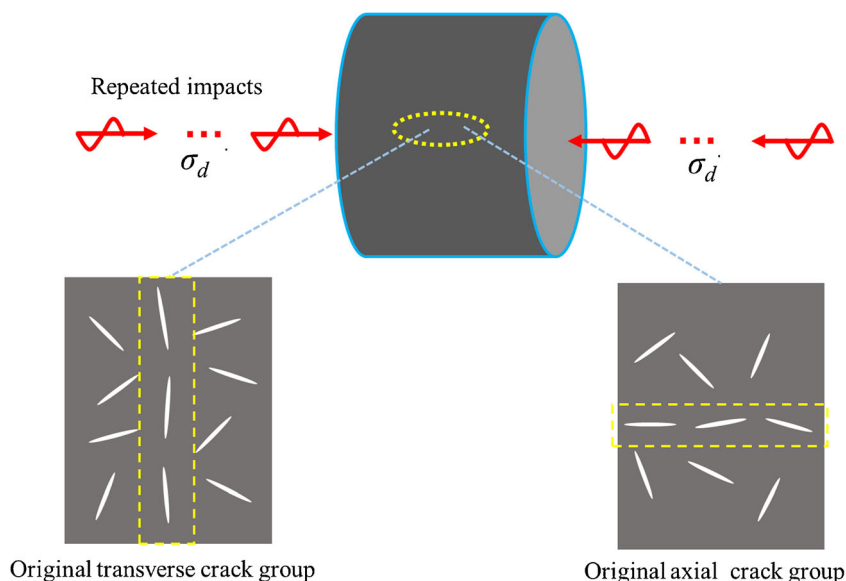
Fig. 14 Influencing factors of the formation of fractures in coal

Original transverse crack group   Original axial crack group

$$L_i = \int_0^t \frac{F_d\sin\theta - K_{ID}^d\sqrt{w\sin\left[\pi(l+l^*)/w\right]}}{F_d\sin\theta - 0.75K_{ID}^d\sqrt{w\sin\left[\pi(l+l^*)/w\right]}} v_R dt \quad (10)$$

$$L_i = \int_0^t \frac{\sigma\sqrt{2w\tan(\pi c/2w)} - K_{ID}^d}{\sigma\sqrt{2w\tan(\pi c/2w)} - 0.75K_{ID}^d} v_R dt \quad (11)$$

Then, the total length of the cracks that propagate during the whole process of the repeated impact test is written as L_{sum}, which can be expressed by Eq. (12).

$$L_{sum} = \sum_{i=1}^{i} L_i \quad (12)$$

On the one hand, when the dynamic stress intensity factor (K_{ID}) of the crack tip reaches the dynamic fracture toughness K_{ID}^d, the cracks start to grow. On the other hand, when L_{sum} reaches the critical length (L_c) between crack groups, the

specimen begins to fail. Therefore, the failure criteria of the axial crack group model and the transverse crack group model under repeated impact loads can be established as follows:

$$\begin{cases} K_{ID} \geq K_{ID}^d \\ L_{sum} = L_c \end{cases} \quad (13)$$

Fracture mechanism of coal under repeated impact loads

According to the failure criteria of the crack group models established above, the whole failure process of coal specimens under repeated impact loads can be explained as follows:

(1) During the impact loading process, part of the stress waves inside the coal body are reflected to form tensile stress waves. Under the action of tensile stress waves, the dynamic stress intensity factor (K_{ID}) at the tip of the

Fig. 15. Crack propagation failure models: **a** axial crack group propagation model, **b** transverse crack group propagation model, **c** force diagram of these models

(a)   (b)   (c)

(a) The process of axial tensile failure

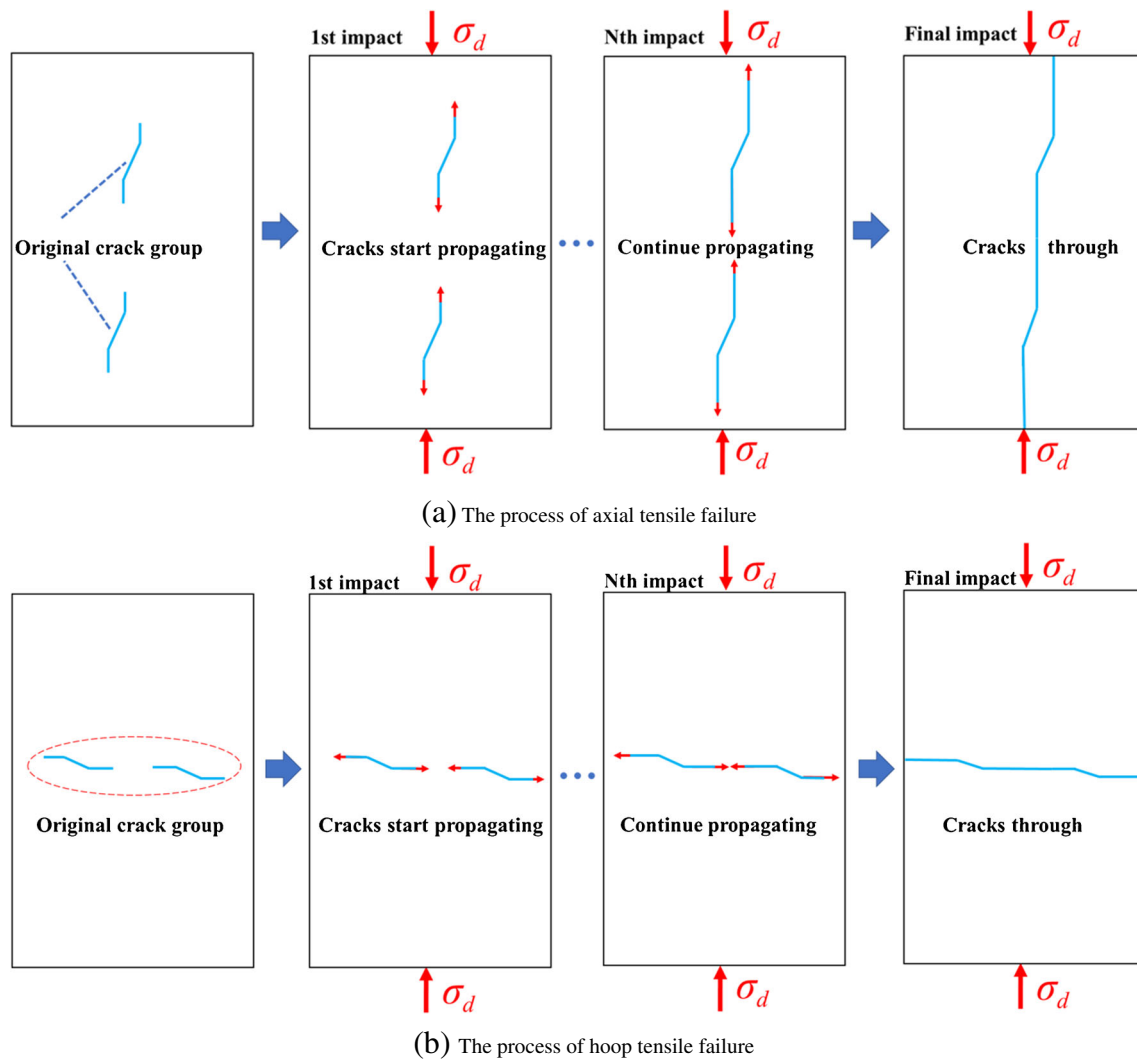(b) The process of hoop tensile failure
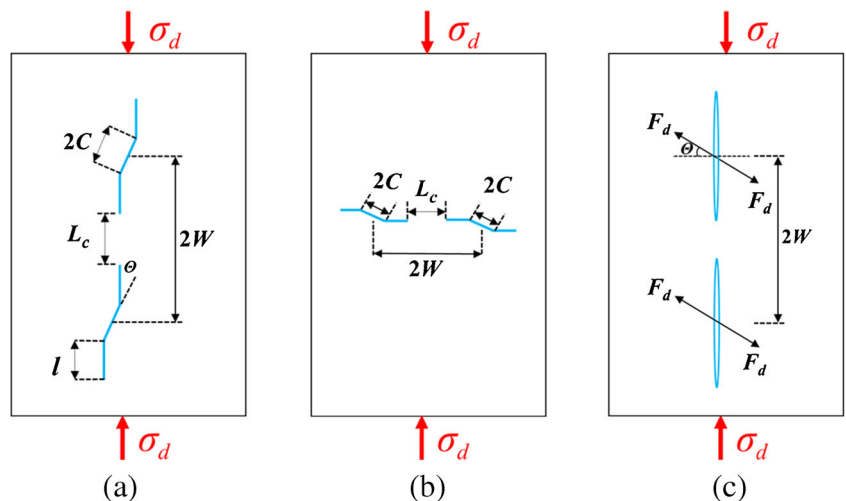
Fig. 16 Failure process of coal under repeated impact loads. (a) The process of axial tensile failure. (b) The process of hoop tensile failure

original transverse crack group reaches the dynamic fracture toughness (K_{ID}^d), and the cracks begin to expand. Then, the length of cracks that are generated after the first impact continues to increase with the increase in the number of impacts. Once the total length (L_{sum}) of the cracks reaches the critical length (L_c), hoop tensile failure of the specimen occurs. The whole process of hoop tensile failure is depicted in Fig. 16(a).

(2) In addition, the coal sample inevitably undergoes lateral expansion due to the Poisson effect (Alawneh et al. 2007). This causes the stress concentration to occur at the tip of the axial crack group. When the dynamic stress intensity factor (K_{ID}) at the tip of the original axial crack group reaches the dynamic fracture toughness (K_{ID}^d), the cracks begin to expand. Then, the tensile cracks that are generated after the first impact continue to expand with an increasing number of impacts. When the total length (L_{sum}) of the cracks reaches the critical length (L_c), macroscopic fracture of the specimen is eventually

generated. The whole process of axial tensile failure is depicted in Fig. 16(b).

Conclusions

In this study, the dynamic mechanical characteristics and fracture mechanism of coal under repeated impact loads are investigated. The main conclusions are as follows:

(1) The dynamic characteristics of coal, such as its dynamic strength and peak strain, are closely related to the number of impacts. As the number of impacts increases, the dynamic strength decreases but the peak strain increases, which indicates that the damage degree of coal specimens can gradually increase under repeated impact loads. It also reveals that frequently dynamic

disturbances can deteriorate the bearing capacity of coal and even induce the instability of coal pillars.

(2) Coal has an obvious characteristic of nonlinear deformation under repeated impact loads, and the strain rebound phenomenon exists in the response of the first impact. However, the slope of the curve in the inelastic deformation phase decreases gradually with increasing impact number, and the phenomenon of strain rebound correspondingly disappears.

(3) Under repeated impact loads, coal specimens present two typical fracture modes: the axial tensile failure mode and hoop tensile failure mode. The original axial crack group and transverse crack group inside the coal are the internal influencing factors, while the repeated impact loads are the external influencing factors. These two main factors ultimately affect the fracture mode of coal, and two crack group failure models are established based on these factors to reveal the fracture mechanism of coal under repeated impact loads.

Declarations

Conflict of interest The authors declare that they have no competing interests.

References

Alawneh AS, Nusier OK, Sharo AA (2007) Poisson's ratio effect on compressive and tensile shaft capacity of driven piles in sand: theoretical formulation. Comput Geotech 34(3):151–163. https://doi.org/10.1016/j.compgeo.2006.11.004

Bai JW, Feng GR, Wang ZH, Wang SY, Qi TY, Wang PF (2019) Experimental investigations on the progressive failure characteristics of a sandwiched coal-rock system under uniaxial compression. Appl Sci-Basel 9(6). https://doi.org/10.3390/app9061195

Cai X, Zhou ZL, Du XM (2020) Water-induced variations in dynamic behavior and failure characteristics of sandstone subjected to simulated geo-stress. Int J Rock Mech Min Sci 130:104339. https://doi.org/10.1016/j.ijrmms.2020.104339

Cao AY, Dou LM, Wang CB, Yao XX, Dong JY, Gu Y (2016) Microseismic precursory characteristics of rock burst hazard in mining areas near a large residual coal pillar: a case study from Xuzhuang coal mine, Xuzhou, China. Rock Mech Rock Eng 49:4407–4422. https://doi.org/10.1007/s00603-016-1036-7

Cording EJ, Hashash YMA, Oh J (2015) Analysis of pillar stability of mined gas storage caverns in shale formations. Eng Geol 184:71–80. https://doi.org/10.1016/j.enggeo.2014.11.001

Dai F, Huang S, Xia KW, Tan Z (2010) Some fundamental issues in dynamic compression and tension tests of rocks using split Hopkinson pressure bar. Rock Mech Rock Eng 43(6):657–666. https://doi.org/10.1007/s00603-010-0091-8

Davies E, Hunter S (1963) The dynamic compression testing of solids by the method of the split Hopkinson pressure bar. J Mech Phys Solids 11(3):155–179. https://doi.org/10.1016/0022-5096(63)90050-4

Freund LB (1990) Dynamic fracture mechanics. Cambridge University Press, London, UK

Horii H, Nemat-Nasser S (1985) Compression induced microcrack growth in brittle solids: axial splitting and shear failure. J Geophys Res 90:3105–3125. https://doi.org/10.1029/JB090iB04p03105

Horii H, Nemat-Nasser S (1986) Brittle failure in compression: splitting, faulting, and brittle-ductile transition. Phil Trans R Soc London 319: 337–374. https://doi.org/10.1098/rsta.1986.0101

ISRM, International Society for Rock Mechanics (1978) Commission on Standardization of Laboratory and Field Tests. Suggested methods for determining tensile strength of rock materials. Int J Rock Mech Min Sci Geomech Abstr 15:99–103

Jin JF, Li XB, Yin ZQ, Du K (2012) Effects of axial pressure and number of cyclic impacts on dynamic mechanical characteristics of sandstone. J China Coal Soc 37(6):920–930

Jin JF, Li XB, Yin ZQ, Yin TB (2013) Effects of axial compression and confining pressure on energy dissipation of sandstone under cyclic impact loads. Rock Soil Mech 34(11):3096–3109. https://doi.org/10.16285/j.rsm.2013.11.007

Jin JF, Li XB, Qiu C, Tao W, Zhou XJ (2014) Evolution model for damage accumulation of rock under cyclic impact loadings and effect of static loads on damage evolution. Chinese J Rock Mech Rock Eng 33(08):1662–1671

Klepaczko J, Hsu T, Bassim M (1984) Elastic and pseudoviscous properties of coal under quasi-static and impact loadings. Can Geotech 21(2):574–583. https://doi.org/10.1139/t84-024

Kong XG, Wang EY, Li SG, Lin HF, Zhang ZB, Ju YQ (2019) Dynamic mechanical characteristics and fracture mechanism of gas-bearing coal based on SHPB experiments. Theor Appl Fract Mech 105: 102395. https://doi.org/10.1016/j.tafmec.2019.102395

Li HB, Zhao J, Li TJ (2000) Micromechanical modelling of the mechanical properties of a granite under dynamic uniaxial compressive loads. Int J Rock Mech Min Sci 37:923–935. https://doi.org/10.1016/S1365-1609(00)00025-3

Li XB, Lok TS, Zhao J (2005) Dynamic characteristics of granite subjected to intermediate loading rate. Rock Mech Rock Eng 38(1):21–39. https://doi.org/10.1007/s00603-004-0030-7

Li XB, Zhou ZL, Lok TS, Hong L, Yin TB (2008) Innovative testing technique of rock subjected to coupled static and dynamic loads. Int J Rock Mech Min Sci 45:739–748. https://doi.org/10.1016/j.ijrmms.2007.08.013

Li HB, Xia X, Li JC, Zhang J, Liu B, Liu YQ (2011) Rock damage control in bedrock blasting excavation for a nuclear power plant. Int J Rock Mech Min Sci 48(2):210–218. https://doi.org/10.1016/j.ijrmms.2010.11.016

Li CW, Wang QF, Lyu PY (2016) Study on electromagnetic radiation and mechanical characteristics of coal during an SHPB test. J Geophys Eng 13:391–398. https://doi.org/10.1088/1742-2132/13/3/391

Li SH, Zhu WC, Niu LL, Yu M, Chen CF (2018) Dynamic characteristics of green sandstone subjected to repetitive impact loading: phenomena and mechanisms. Rock Mech Rock Eng 51:1921–1936. https://doi.org/10.1007/s00603-018-1449-6

Mohr D, Gary G, Lundberg B (2010) Evaluation of stress-strain curve estimates in dynamic experiments. Int J Impact Eng 37:161–169. https://doi.org/10.1016/j.ijimpeng.2009.09.007

Ramulu M, Chakraborty AK, Sitharam TG (2009) Damage assessment of basaltic rock mass due to repeated blasting in a railway tunneling project - a case study. Tunn Undergr Sp Tech 24:208–221. https://doi.org/10.1016/j.tust.2008.08.002

Shan RL, Cheng RQ, Gao WJ (2006) Study on dynamic constitutive model of anthracite of Yunjialing coal mine. Chinese J Rock Mech Rock Eng 25(11):2258–2263

Shu RH, Yin TB, Li XB, Yin ZQ, Tang LZ (2019) Effect of thermal treatment on energy dissipation of granite under cyclic impact loading. T Nonferr Metal Soc 29:385–396. https://doi.org/10.1016/S1003-6326(19)64948-4

Tang LZ, Wang C, Cheng L, Gao LH (2015) Experimental study of mechanical characteristics of skarn under one-dimensional coupled static and cyclic impact loads. J Cent South Univ 46(10):3898–3908. https://doi.org/10.11817/j.issn.1672-7207.2015.10.045

Wang E, Shrive N (1995) Brittle fracture in compression: mechanics, models and criteria. Eng Fract Mech 52(6):1107–1126. https://doi.org/10.1016/j.tafmec.2018.08.014

Wang SY, Sloan SW, Huang ML, Tang CA (2011) Numerical study of failure mechanism of serial and parallel rock pillars. Rock Mech Rock Eng 44:179–198. https://doi.org/10.1007/s00603-010-0116-3

Wang W, Li HM, Yuan RF, Gu HL, Wang C, Li HG (2016) Micromechanics analysis and mechanical characteristics of water-saturated coal samples under coupled static-dynamic loads. J China Coal Soc 41(3):611–617. https://doi.org/10.13225/j.cnki.jccs.2015.0558

Wang C, Tang LZ, Cheng L (2017) Damage characteristics and constitutive model of rock under three-dimensional high static load and frequent dynamic disturbance. Rock Soil Mech 38(08):2286–2305. https://doi.org/10.16285/j.rsm.2017.08.017

Wang G, Guo YY, Wang PF, Li WX, Wu MM, Sun LL, Cao JJ, Du CG (2020) A new experimental apparatus for sudden unloading of gas-bearing coal. B Eng Geol Environ 79:857–868. https://doi.org/10.1007/s10064-019-01601-3

Wong LNY, Einstein HH (2009a) Crack coalescence in molded gypsum and Carrara marble: part 1-macroscopic observations and interpretation. Rock Mech Rock Eng 42(3):475–511. https://doi.org/10.1007/s00603-008-0002-4

Wong LNY, Einstein HH (2009b) Crack coalescence in molded gypsum and Carrara marble: part 2-microscopic observations and interpretation. Rock Mech Rock Eng 42(3):513–545. https://doi.org/10.1007/s00603-008-0003-3

Xia KW, Yao W (2015) Dynamic rock tests using split Hopkinson (Kolsky) bar system – a review. J. Rock Mech Rock Eng 7:27–59. https://doi.org/10.1016/2847j.jrmge.2014.07.008

Xiao JQ, Ding DX, Xu G, Jiang FL (2009) Inverted S-shaped model for nonlinear fatigue damage of rock. Int J Rock Mech Min Sci 46:643–648. https://doi.org/10.1016/j.ijrmms.2008.11.002

Xu JM, Zhu WB, Ju JF (2017) Mechanism of dynamic mine pressure occurring below adjacent upper chamber mining goaf with shallow cover depth. J China Coal Soc 42:500–509. https://doi.org/10.13225/j.cnki.Jccs.2016.0811

Yang JX, Liu CY, Yu B, Wu FF (2015) The effect of a multi-gob, pier-type roof structure on coal pillar load-bearing capacity and stress distribution. B Eng Geol Environ 74:1267–1273. https://doi.org/10.1007/s10064-014-0685-6

Yin TB, Peng K, Wang L, Wang P, Yin XY, Zhang YL (2016) Study on impact damage and energy dissipation of coal rock exposed to high temperatures. Shock Vib 2016:5121932–5121910. https://doi.org/10.1155/2016/5121932

Yin ZQ, Chen WS, Hao H, Chang JC, Zhao GM, Chen ZY, Peng K (2019) Dynamic compressive test of gas-containing coal using a modified split Hopkinson pressure bar system. Rock Mech Rock Eng 53:815–829. https://doi.org/10.1007/s00603-019-01955-w

Zhang QB, Zhao J (2014) A review of dynamic experimental techniques and mechanical behaviour of rock materials. Rock Mech Rock Eng 47:1411–1478. https://doi.org/10.1007/s00603-013-0463-y

Zhang YJ, Feng GR, Zhang M, Ren HR, Bai JW, Guo YX, Jiang HN, Kang LX (2016) Residual coal exploitation and its impact on sustainable development of the coal industry in China. Energy Policy 96:534–541. https://doi.org/10.1016/j.enpol.2016.06.033

Zhang XQ, Gong PL, Wang K, Li JZ, Jiang YL (2019) Characteristic and mechanism of roof fracture ahead of the face in an LTCC panel when passing an abandoned roadway: a case study from the Shenghua Coal Mine, China. Rock Mech Rock Eng 52:2775–2778. https://doi.org/10.1007/s00603-019-01751-6

Zhao YX, Liu SM, Jiang YD, Wang K, Huang YQ (2016) Dynamic tensile strength of coal under dry and saturated conditions. Rock Mech Rock Eng 49:1709–1720. https://doi.org/10.1007/s00603-015-0849-0

Zhou YX, Xia K, Li XB, Li HB, Ma GW, Zhao J, Zhou ZL, Dai F (2012) Suggested methods for determining the dynamic strength parameters and mode-I fracture toughness of rock materials. Int J Rock Mech Min Sci 49:105–112. https://doi.org/10.1016/j.ijrmms.2011.10.004

Zhou ZL, Chen L, Cai X, Shen BT, Zhou J, Dun K (2018) Experimental investigation of the progressive failure of multiple pillar-roof system. Rock Mech Rock Eng 51:1629–1636. https://doi.org/10.1007/s00603-018-1441-1

Zhu JJ, Li XB, Gong FQ, Wang SM (2013) Dynamic characteristics and damage model for rock under uniaxial cyclic impact compressive loads. Chinese J Geotech Eng 35(3):531–539

Zhu WB, Xu JL, Li YC (2017) Mechanism of the dynamic pressure caused by the instability of upper chamber coal pillars in Shendong coalfield, China. Geosci J 21:729–741. https://doi.org/10.1007/s12303-017-0025-5